

Identification of Compounds with Potential Antibacterial Activity against *Mycobacterium* through Structure-Based Drug Screening

Tomohiro Kinjo,^{†,⊥} Yuji Koseki,^{†,⊥} Maiko Kobayashi,[†] Atsumi Yamada,[†] Koji Morita,[†] Kento Yamaguchi,[†] Ryoya Tsurusawa,[†] Gulcin Gulten,[‡] Hideyuki Komatsu,[†] Hiroshi Sakamoto,[†] James C. Sacchettini,[‡] Mitsuru Kitamura,[§] and Shunsuke Aoki^{*,†,||}

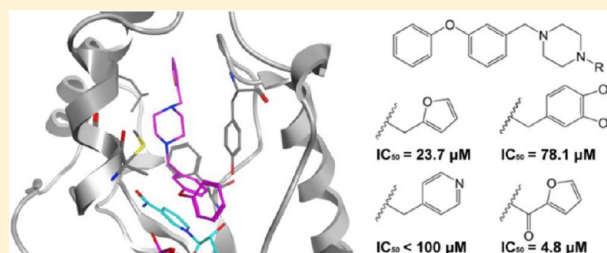
[†]Department of Bioscience and Bioinformatics, Graduate School of Computer Science and Systems Engineering, Kyushu Institute of Technology, 680-4 Kawazu, Iizuka-shi, Fukuoka 820-8502, Japan

[‡]Department of Biochemistry & Biophysics, Texas A&M University, College Station, Texas 77843-2128, United States

[§]Department of Applied Chemistry, Kyushu Institute of Technology, 1-1 Sensui-cho, Tobata, Kitakyushu 804-8550, Japan

^{||}Biomedical Informatics Research and Development Center (BMIRC), Kyushu Institute of Technology, 680-4 Kawazu, Iizuka-shi, Fukuoka 820-8502, Japan

ABSTRACT: To identify novel antibiotics against *Mycobacterium tuberculosis*, we performed a hierarchical structure-based drug screening (SBDS) targeting the enoyl-acyl carrier protein reductase (InhA) with a compound library of 154,118 chemicals. We then evaluated whether the candidate hit compounds exhibited inhibitory effects on the growth of two model mycobacterial strains: *Mycobacterium smegmatis* and *Mycobacterium vanbaalenii*. Two compounds (KE3 and KE4) showed potent inhibitory effects against both model mycobacterial strains. In addition, we rescreened KE4 analogs, which were identified from a compound library of 461,383 chemicals through fingerprint analysis and genetic algorithm-based docking simulations. All of the KE4 analogs (KES1–KES5) exhibited inhibitory effects on the growth of *M. smegmatis* and/or *M. vanbaalenii*. Based on the predicted binding modes, we probed the structure–activity relationships of KE4 and its analogs and found a correlative relationship between the IC_{50} values and the interaction residues/LogP values. The most potent inhibitor, compound KES4, strongly and stably inhibited the long-term growth of the model bacteria and showed higher inhibitory effects ($IC_{50} = 4.8 \mu\text{M}$) than isoniazid ($IC_{50} = 5.4 \mu\text{M}$), which is a first-line drug for tuberculosis therapy. Moreover, compound KES4 did not exhibit any toxic effects that impede cell growth in several mammalian cell lines and enterobacteria. The structural and experimental information of these novel chemical compounds will likely be useful for the development of new anti-TB drugs. Furthermore, the methodology that was used for the identification of the effective chemical compound is also likely to be effective in the SBDS of other candidate medicinal drugs.



INTRODUCTION

Mycobacterium tuberculosis (*M. tuberculosis*), which is an infecting agent of tuberculosis (TB), is a serious worldwide menace. The World Health Organization has estimated that more than one-third of the world's population is infected by *M. tuberculosis* and that 1.7 million of these infections result in death each year.¹ The coinfection of Human Immunodeficiency Virus (HIV) with TB is a significant factor that increases the morbidity rate of this disease.^{1,2} In addition, the infections of multidrug-resistant TB (MDR-TB) and extensively drug-resistant TB (XDR-TB) are rapidly spreading worldwide.¹ To counteract the global drug resistance problems of TB, there is an urgent need to identify new drugs to combat these resistant TBs.

The widely used treatments for TB involve the administration of a combination of curative drugs. One of the most effective and specific of these curative drugs is isoniazid (INH), which is a pro-drug and must be activated by the mycobacterial

catalase peroxidase (KatG) to form the INH-NAD adduct.^{3,4} This adduct inhibits the enoyl-acyl carrier protein (ACP) reductase (InhA), which is involved in the mycobacterial type II fatty acid biosynthesis pathway (FAS- II).^{5–7} In this pathway, the InhA enzyme plays a major role in the synthesis of mycolic acid, which is a major component of the cell wall and is essential for the growth of *Mycobacterium*.^{8,9} Therefore, the inhibition of the activity of InhA blocks mycolic acid biosynthesis and ultimately leads to the cellular death of *Mycobacterium*. However, the duration of the INH administration is limited due to its hepatotoxicity.¹⁰ Because it has been reported that the causes of resistance to INH are mutations of KatG and InhA, it is necessary to develop new chemical compounds that directly inhibit InhA and do not

Received: December 3, 2012

interact with the mutated residues of InhA in MDR- and XDR-TBs.^{11–13}

High-throughput screening (HTS) is the traditionally predominant method that is used to identify lead compounds for new drugs. Although HTS is able to identify hit (active) compounds from large-scale physical libraries of compounds, it is an expensive undertaking in terms of mustering the chemical compounds and organizing the assay results. Currently, the *in silico* screening approach is considered one of the powerful methods for the rapid discovery of novel lead compounds with potential activity. This approach is cost-effective and enables the understanding of the binding mode and the obtaining of additional information that would aid the optimization of the hit compounds. *In silico* drug screening can be divided into two approaches. One of these is ligand-based drug screening, which includes the quantitative structure–activity relationship (QSAR) method,¹⁴ screening with pharmacophore models,¹⁵ and 2D chemical¹⁶/3D shape¹⁷ similarity screenings. These screening methods usually use the hit compound activities (EC_{50} , IC_{50} , K_m , or K_i values), actions, and some quantified data of the hit compound–protein interactions. The other approach is structure-based drug screening (SBDS),¹⁸ which is generally used to identify hit compounds from virtual large-scale compound libraries using docking simulation tools, such as DOCK,¹⁹ AutoDock,²⁰ GOLD,^{21,22} and GLIDE.²³ A further advantage can be gained through the use of at least two of these tools in the screening process. In previous studies, we identified active compounds against various crystal structures through the use of both DOCK and GOLD.^{24–26} These previous studies indicated the efficacy of the DOCK-GOLD chain SBDS method, and we also recently proposed a novel DOCK-GOLD chain SBDS method with multiple chemical conformers.²⁷ In this study, we used an additional fingerprint method followed by the DOCK-GOLD chain SBDS method to identify hit compounds and their analogs that have activity against *M. tuberculosis* InhA. The screening of the ChemBridge compound library,²⁸ which contains 154,118 compounds, yielded two hits, which were able to inhibit the growth of mycobacteria *in vitro*. We also used similarity analysis to identify five additional compounds that have similar structures to the first hit compound from a ChemBridge compound library that contains 461,383 compounds. Our subsequent computational and experimental analyses identified two active compounds (*Mycobacterium smegmatis*: KE4 IC_{50} = 23.7 μ M and KES4 IC_{50} = 4.8 μ M) that did not exhibit any toxicity in intestinal bacteria models and mammalian cell models. Moreover, we experimentally demonstrated that these compounds directly inhibit *M. tuberculosis* InhA. Additionally, these compounds are predicted to have relatively low toxic effects toward mammals, as determined by *in silico* toxicity testing. The structural and experimental information for these active compounds will contribute to the development of anti-TB medical drugs.

RESULTS

DOCK and GOLD Screening. The active center cavity of InhA is composed of the substrate-binding loop (residues 195–210) and the following residues: Gly14, Thr17, Ser20, Ile21, Ala22, Ser94, Ser149, Met155, Tyr158, Lys165, Ile194, Met199, and Leu218 (Figure 1).^{29,30} To generate the protein surface and to determine the docking simulation area, we used the DMS¹⁹ and the SPHGEN¹⁹ programs. We performed a three-step screening process using DOCK (first screening) and

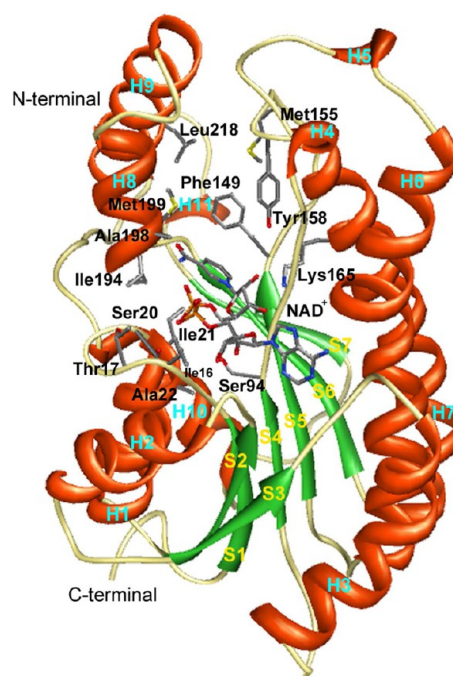


Figure 1. Three-dimensional structure of *M. tuberculosis* InhA in complex with its NAD^+ cofactor. The secondary structures are indicated by ribbon representations [α -helix (H1–H11): orange, β -sheet (S1–S7): green]. The amino acid residues of the active site are shown as a stick model.

GOLD (second screening: single conformation, third screening: multiconformation) (Figure 2A). In the DOCK screening, we used the ChemBridge library that contains 154,118 chemical compounds. This DOCK screening identified the top 2,000 ranked chemical compounds (1.3% of the primary chemical compound library) that had energy scores of less than -49.7 kcal/mol. The calculation speed of the DOCK-based screening is very fast because of the grid-based calculations without hydrogen bond (H-bond) energy by PC clustering. However, the accuracy of the calculations is relatively low (the area under the curve (AUC) values of receiver-operating characteristic (ROC) = 0.56; data not shown). After DOCK screening, the conformations of the top 2,000 compounds were screened again using the GOLD performing genetic algorithm that includes van der Waals, H-bond, and molecular torsion energies (the AUC values of ROC = 0.72; data not shown). We identified the top 1,000 ranked chemical compounds that were obtained from the GOLD screening, which was performed using a single conformation per compound. Those chemical compounds with a GOLD score of more than 85 were used in a third screening. This third screening was performed using 10 conformations per compound, which were generated using the LowMode MD method under the pH 7.0 condition.^{31,32} After the third screening, the top 29 ranked chemical compounds showed GOLD average scores of more than 80. Finally, through clustering using BIT_MACCS fingerprint methods,^{31,33} 5 unique chemical compounds were selected (KE1–KE5, GOLD Scores: 81.66–98.23 (Table 1)).

Bacterial Growth Activity Assay of Compounds KE1–KE5. The 5 selected chemical compounds (KE1–KE5) were assessed for their *in vitro* bacterial growth activity using the model bacteria *M. smegmatis*, *M. vanbaalenii*, and *Rhodococcus opacus* (*R. opacus*). These model bacteria (Biosafety Level 1)

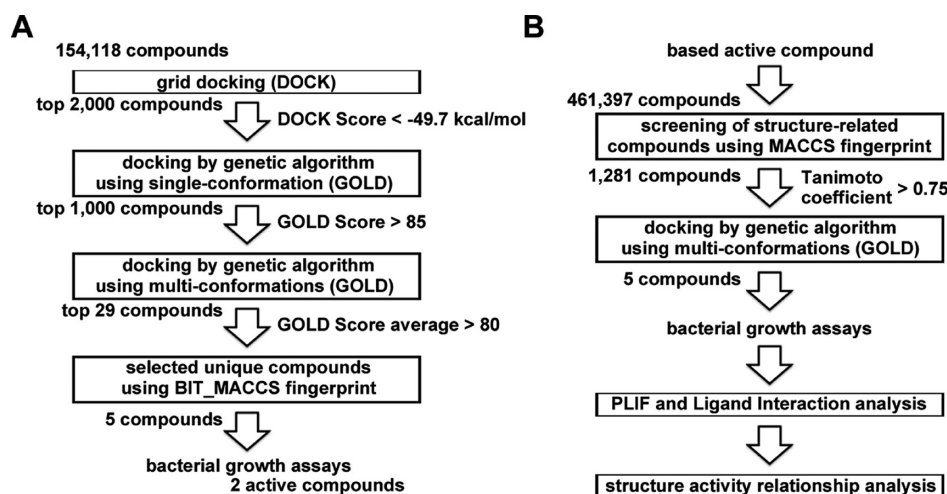


Figure 2. Flowcharts of the SBDS and chemical analog search strategies applied in this study. (A) Flowchart of the candidate chemical compounds obtained through the three-step *in silico* SBDS. (B) Flowchart of the identification of the analogs of the active compound structure.

Table 1. List of the Five Selected Compounds That Were Identified by the *in Silico* Screening

chemical name	GOLD score ^a
KE1	98.23 ± 0.56
KE2	94.95 ± 0.82
KE3	88.44 ± 0.55
KE4	82.14 ± 0.11
KE5	81.66 ± 0.58

^aEach value represents the mean ± SEM.

have highly and moderately conserved amino acid sequences of InhAs: 87%, 86%, and 65% similarity between the *M. smegmatis*, *M. vanbaalenii*, and *R. opacus* InhAs compared with the *M. tuberculosis* InhA.³⁴ The candidate chemical compounds (at a concentration of 50 μ M) that were identified by the *in silico* screening process were tested to determine their inhibitory effects on the growth of *M. smegmatis* and *M. vanbaalenii*. Two of the five chemical compounds, KE3 and KE4 (50 μ M), strongly inhibited the growth of both *M. smegmatis* and *M. vanbaalenii* after 24 h (Figures 3A and 3B). In contrast, compounds KE1, KE2, and KE5 failed to inhibit the growth of both model bacteria (Figures 3A and 3B). The chemical structures of compounds KE3 and KE4 are shown in Figure 4A. We also performed a long-term bacterial growth assay using *M. smegmatis* and *M. vanbaalenii* to validate the long-term stability and effectiveness of compounds KE3 and KE4 over 72 h. Over the course of the 72 h, compounds KE3 and KE4 (50 μ M) continually inhibited the growth of both bacterial strains at the same level as that obtained with INH (Figures 4B and 4C). In the bacterial growth assay using *R. opacus*, compound KE3 (50 μ M) inhibited the bacterial growth at the same level as INH after 24 h, whereas compound KE4 (50 μ M) exhibited a weak inhibitory effect (Figure 4D).

Enterobacterial Toxicity Assay of Chemical Compounds KE3 and KE4. We performed an enterobacterial toxicity assay using *Escherichia coli* (*E. coli*) as the model bacteria. For the treatment of TB, it is necessary to take a medical drug for a long period of time (one year).³⁵ Thus, we assessed the enterobacterial toxicity of compounds KE3 and KE4. We tested their toxic effect against the *E. coli* JM109 and BL21 strains. Compounds KE3 and KE4 had no toxic effect on

the growth of either strain after 8 h (JM109: data not shown, BL21: Figure 4E).

Mammalian Cell Toxicity Assay for Compounds KE3 and KE4. We then assessed whether the effective compounds KE3 and KE4, which were identified by the bacterial growth assay, have toxic effects on mammalian cells. The mammalian cell toxicity assay was performed using Madin-Darby canine kidney (MDCK) and human neuroblastoma (SH-SY5Y) cells. Compound KE4 had no toxic effects on the cultured mammalian cells, whereas compound KE3 exhibited some toxic effects on both cultured mammalian cells (Figures 5A and 5B).

Screening of Structure-Related Compounds. We performed a rescreening to identify whether other compounds with a similar structure to that of compound KE4 would have higher effectivity (Figure 2B). We initially obtained similar chemical compounds from a Web-based database (Hit2LEAD.com)²⁸ using a similarity search tool that is available on the Web site. In addition, we assembled similar chemical compounds by fingerprint analysis from a larger-scale virtual compound library that contains 461,397 chemical compounds (ChemBridge). Furthermore, we performed GOLD docking simulations using the same process that was used for the identification of compounds KE1–KE5. As a result, we identified 5 structurally similar chemical compounds (KES1–KES5) that have equal or higher GOLD score averages than that of KE4. The structures of KES1–KES5 are shown in Table 2. The compounds KE4 and KES1–KES5 have a piperidine ring as a common scaffold. The piperidine ring has a variety of protonation states under different pH conditions. In this study, compound protonation states were configured at pH 7.0 using the Protonate 3D module in MOE because this pH suits the conditions of several conventional *in vitro* assays. As a result, all compounds (KE4 and KES1–KES5) had the same protonation state, which is shown in the scaffold structure of Table 2.

Bacterial Growth Activity Assay of Compounds KES1–KES5. We performed an *in vitro* bacterial growth activity assay (50 and 100 μ M) to test whether these newly identified chemical compounds actually inhibit bacterial growth. The compounds KES1 (50 μ M) and KES4 (50 μ M) completely inhibited the growth of *M. smegmatis* after 24 h (Figure 6A). The chemical compounds KES2 (100 μ M: data not shown), KES3 (50 μ M: Figure 6A), and KES5 (100 μ M:

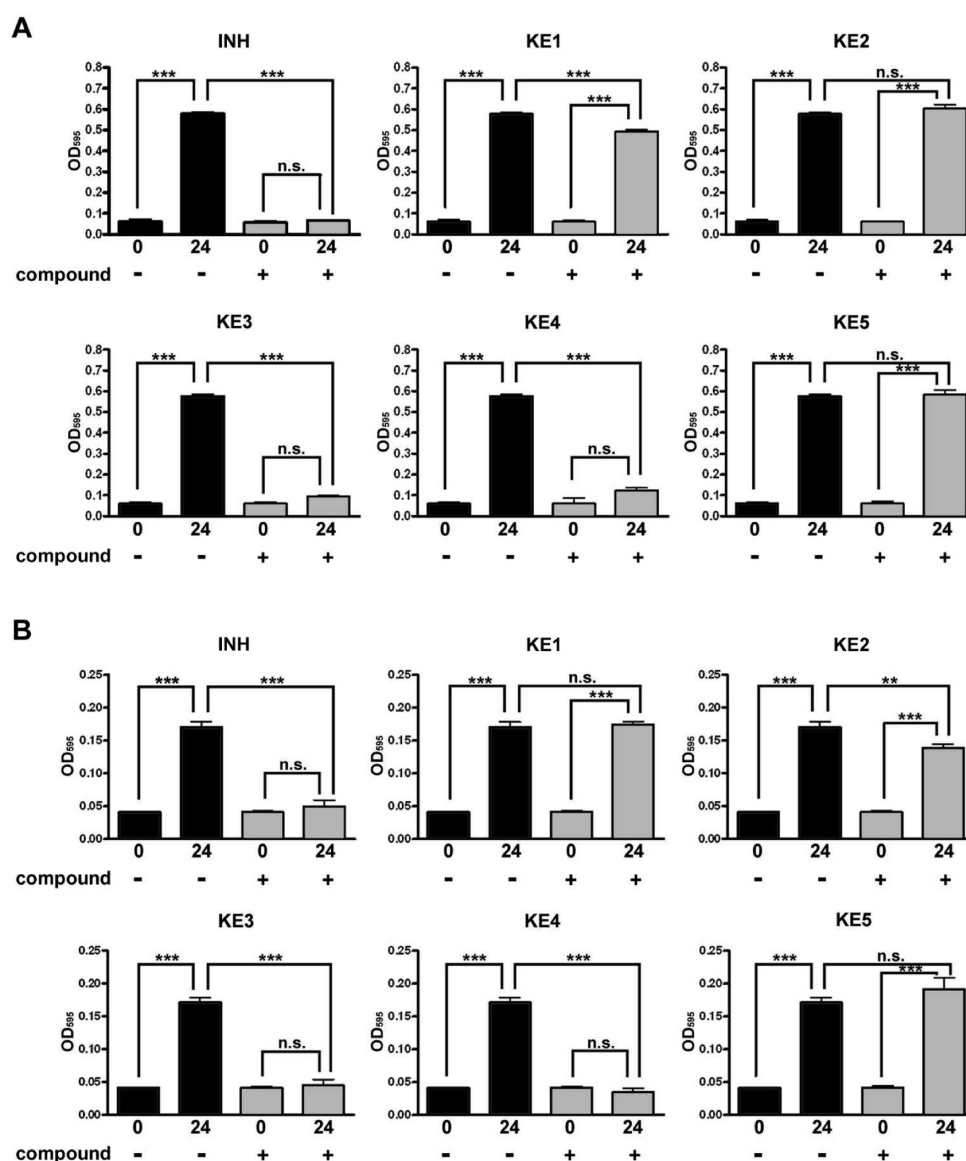


Figure 3. Short-term (24 h) inhibitory effects of the candidate chemicals (KE1–KE5) on the growth of the model mycobacteria: (A) *M. smegmatis* and (B) *M. vanbaalenii*. The chemical compounds were added to the cultures at a concentration of 50 μ M. DMSO (0.3%) and INH (50 μ M) were used as the negative and positive controls, respectively. Each value represents the mean \pm SEM of four independent experiments. Bonferroni's all pair comparison tests were performed (n.s. not significant, ** p < 0.01, *** p < 0.001).

data not shown) showed weak inhibitory effects on *M. smegmatis* growth. The compound KES3 (100 μ M: data not shown) completely inhibited the growth of *M. smegmatis*. In addition, all of the compounds (KES1–KES5: 50 μ M) completely inhibited the growth of *M. vanbaalenii* (Figure 6B). Thus, the compounds KES1, KES3, and KES4 inhibited the growth of both model bacteria. In addition, we performed a long-term bacterial growth assay using *M. smegmatis* and *M. vanbaalenii* to validate the long-term stability and effectiveness of compounds KES1, KES3, and KES4 over 72 h. The compounds KES1 and KES4 (50 μ M) continuously inhibited the growth of *M. smegmatis* after 72 h; this effect was similar to that obtained with INH (Figure 7A). Although compound KES3 at a concentration of 50 μ M was not able to successfully inhibit the long-term growth of this bacteria (Figure 7A), a higher concentration of the compound (100 μ M: data not shown) showed satisfactory inhibitory effects. However, similarly to INH, the KE4 analog compounds (KES1, KES3

and KES4: 50 μ M) inhibited the growth of *M. vanbaalenii* after 72 h (Figure 7B). In the bacterial growth assay using *R. opacus*, all of the compounds (KES1, KES3, and KES4: 50 μ M) showed weak inhibitory effects on the growth of the bacteria, whereas INH (50 μ M) completely inhibited it (Figure 7C).

Enterobacterial Toxicity Assay of Compounds KES1–KES5. We performed an enterobacterial toxicity assay and found that compounds KES1 and KES4 had no toxic effect on the growth of both strains that were tested (Figure 7D). However, compound KES3 exhibited a weak toxic effect on both strains (JM109: data not shown, BL21: Figure 7D).

Mammalian Cell Toxicity Assay of Compounds KES1–KES5. We performed a mammalian cell toxicity assay with compounds KES1, KES3, and KES4. These compounds were added to mammalian cell cultures (MDCK and SH-SY5Y cells) to test their cytotoxicity. Compounds KES4 had no toxic effects on these cultured mammalian cells, whereas compound KES1

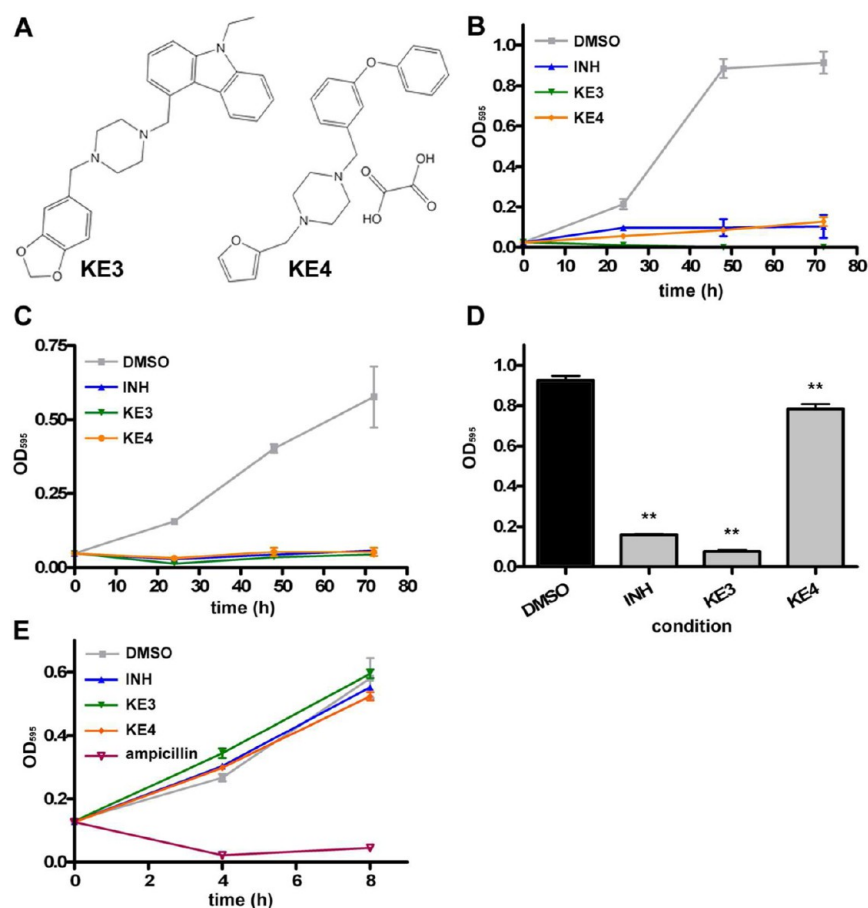


Figure 4. The validation of the stability and specificity of the active compounds. (A) Chemical structures of the active hits identified by SBDS. Effects of the chemical compounds on the long-term (~72 h) growth of the model mycobacteria: (B) *M. smegmatis* and (C) *M. vanbaalenii*. Effects of the chemical compounds (50 μ M) on the growth of (D) *R. opacus* and (E) enterobacteria (*E. coli* BL 21; ~8 h). DMSO (0.3%) and INH (50 μ M) were used as the negative and positive controls, respectively. The concentration of ampicillin that was used was 100 μ g/mL. Each value represents the mean \pm SEM of four independent experiments. Dunnett's multiple comparison tests were performed to analyze the data in (D). The statistical significance is indicated (** $p < 0.01$).

and KES3 had some toxic effects on either cultured mammalian cells (Figures 8A and 8B).

In Silico Estimation of Oral LD₅₀ in Rats. We predicted the oral LD₅₀ values in rats using an *in silico* estimation tool, TEST (Toxicity Estimation Software Tool). It has been reported that this LD₅₀ model reliably predicts oral LD₅₀ values in rats.³⁶ The LD₅₀ value of INH and rifampicin (RFP), first-line drugs against TB, were included in the training set because their experimental LD₅₀ values are already known (9.12×10^{-3} mol/kg and 1.91×10^{-3} mol/kg, respectively). The candidate chemicals (KE4 and KES1–KES5) were predicted to have LD₅₀ values of 3.98×10^{-3} mol/kg (KE4), 2.88×10^{-3} mol/kg (KES1), 1.91×10^{-3} mol/kg (KES2), 2.24×10^{-3} mol/kg (KES3), 2.57×10^{-3} mol/kg (KES4), and 2.09×10^{-3} mol/kg (KES5). The LD₅₀ values of the candidate chemicals are higher than that of RFP but lower than that of INH.

Determination of IC₅₀ Value. We examined the dose-dependent effects of INH, compound KE4, and compounds KES1–KES5 on the growth of *M. smegmatis*. The experimentally determined IC₅₀ values of these compounds for *M. smegmatis* were 5.4 μ M (INH; data not shown), 23.7 μ M (KE4), 78.1 μ M (KES1), <100 μ M (KES2), <100 μ M (KES3), 4.8 μ M (KES4), and >100 μ M (KES5) (Figures 9A–9F). The inhibitory effects of these chemical compounds on the growth

of *M. smegmatis* were lower than for their effects on the growth of *M. vanbaalenii* (data not shown). However, it is noteworthy that the IC₅₀ value of KES4 is less than that of INH (5.4 μ M).

***M. tuberculosis* InhA Enzymatic Assay.** To address whether the three chemicals (KE4, KES1, and KES4) that had IC₅₀ values lower than 100 μ M affect the enzymatic activity of *M. tuberculosis* InhA, enzymatic assays were performed using 2-*trans*-decanoyl CoA as a model substrate. Triclosan (TCS, experimentally determined K_i value = 0.2 μ M) was used as a positive control.³⁷ All three of the chemicals (KE4, KES1, and KES4) significantly inhibited InhA enzymatic activity (Figure 10) compared to the negative control (DMSO, 0.3%). Notably, KES4 (final concentration: 50 μ M) inhibited InhA enzymatic activity by 85.1% compared to DMSO.

Prediction of Chemical Compound Binding Mode to the Target Protein, *M. tuberculosis* InhA. Figure 11 shows the predicted binding mode of the different chemical compounds that yielded the best GOLD score with the crystal structure of the *M. tuberculosis* InhA. Tyr158 is known to be a natural substrate (ACP substrate)-binding site of *M. tuberculosis* InhA.³⁸ All of the chemical compounds (KE4 and KES1–KES5) were predicted to be located near the substrate-binding site with a mode that would inhibit the bond of the natural substrate. Moreover, using 10 multiconformations, which were obtained from the results of the third screening, we performed

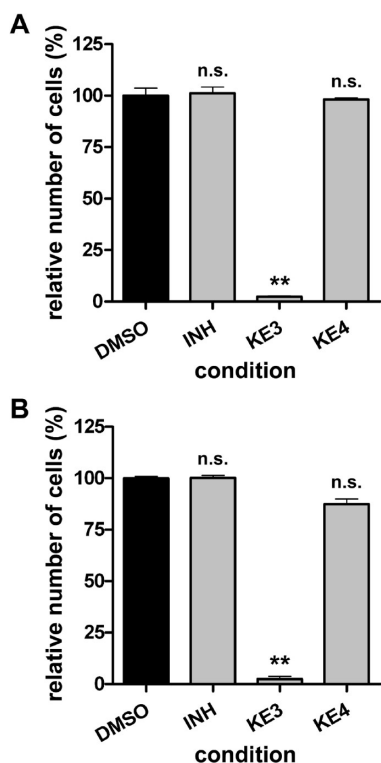
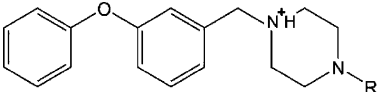
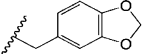
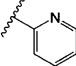
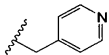
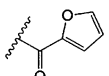
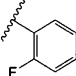


Figure 5. Toxic effects of the chemical compounds (KE3 and KE4) on cultured mammalian cells: (A) MDCK cells and (B) SH-SY5Y cells. The chemical compounds were added to the cultures at a concentration of 30 μ M. Each value represents the mean \pm SEM of four independent experiments. Dunnett's multiple comparison tests were performed. The statistical significance is indicated (n.s. not significant, $**p < 0.01$).

Table 2. KE4 Analogs with Different R Substituents^a

		
Chemical Name	R	GOLD Score*
KES1		87.10 \pm 0.62
KES2		84.78 \pm 0.41
KES3		84.65 \pm 0.82
KES4		83.48 \pm 0.37
KES5		83.20 \pm 0.42

^aThe * denotes the following: each value represents the mean \pm SEM.

a protein–ligand interaction fingerprint (PLIF) analysis³¹ and a Ligand Interaction analysis³¹ to investigate the detailed interactions. All of the tested chemical compounds interact with Leu218, which is located near the active center of the *M. tuberculosis* InhA (Table 3). The 2-furyl group of compound KE4 exhibits a hydrophobic interaction with Leu218. In addition, the piperazine group of KE4 forms a H-bond with Met199, and its 3-phenoxybenzyl group has arene-H and hydrophobic interactions with Phe149 and Ala198 (not shown in the figure), respectively (Figure 11A and Table 3). The analysis of the binding mode of compound KES1 suggested that its benzodioxol group interacts with Ala198 and that its 3-phenoxybenzyl group interacts with Leu218 through a hydrophobic interaction (Figure 11B and Table 3). In the binding mode of compound KES2, its 3-phenoxybenzyl or 2-pyridinyl group forms a hydrophobic interaction with Leu218. In its predicted binding mode that yielded the best GOLD score, compound KES2 forms an H-bond with Met199 (Figure 11C and Table 3). The binding mode of compound KES3 shows a hydrophobic interaction between its 3-phenoxybenzyl group and Leu218 (Figure 11D and Table 3). The compound KES4 has the most stable predicted binding mode: the ring of the 2-furoyl group of KES4 exhibits hydrophobic interactions with Leu218, its 3-phenoxybenzyl group has an arene-H interaction with Phe149, and the oxygen of the 2-furoyl group forms an H-bond with Tyr158 (Figure 11E and Table 3). The 3-phenoxybenzyl group of KES5 forms a hydrophobic interaction with Leu218 (Figure 11F and Table 3).

DISCUSSION

In this study, we identified seven chemical compounds (KE3, KE4, and KES1–KES5) that inhibit the growth of *M. smegmatis* and/or *M. vanbaalenii*. Compounds KE4 and KES4 inhibited the growth of both model *Mycobacterium* strains to a similar extent as INH, and the chemicals directly inhibited *M. tuberculosis* InhA. Moreover, these compounds did not have statistically significant toxic effects on the model enterobacteria (*E. coli*: JM109 and BL21 strains) or mammalian cells (MDCK and SH-SY5Y cells). In addition, the *in silico* estimation of oral LD₅₀ in rats suggested that these compounds have higher LD₅₀ values than INH. In particular, compound KES4 strongly inhibited the growth of *M. smegmatis*. The IC₅₀ value of compound KES4 was found to be 4.8 μ M (Figure 9E), which demonstrates its higher efficacy than that of INH (5.4 μ M; data not shown). It is known that the cell division and elongation mechanisms of *M. smegmatis* resemble those of *M. tuberculosis*;³⁹ thus, it is expected that KES4 will exhibit a similar antibacterial effect against *M. tuberculosis* in future drug research. The information obtained from the analysis of the chemical structure of KES4 is likely to be useful in the development of new anti-TB drugs.

All of the active compounds (KE3, KE4, and KES1–KES5) were predicted to have hydrophobic interactions with the Leu218 residue of the *M. tuberculosis* InhA (Figure 11 and Table 3). It is assumed that the inhibitory effects are increased by hydrophobic interactions with Ala198 (Table 3). Based on the analysis of the data obtained for compounds KE4 and KES4 (Figures 11A and 11E and Table 3), the arene-H interaction with Phe149 may also lead to good inhibitory performance. Furthermore, the H-bond that is formed between compound KES4 and Tyr158 considerably improves the growth inhibitory effect of this compound against *M. smegmatis* (Table 3). Based on our structure–activity relationship (SAR) studies of KE4

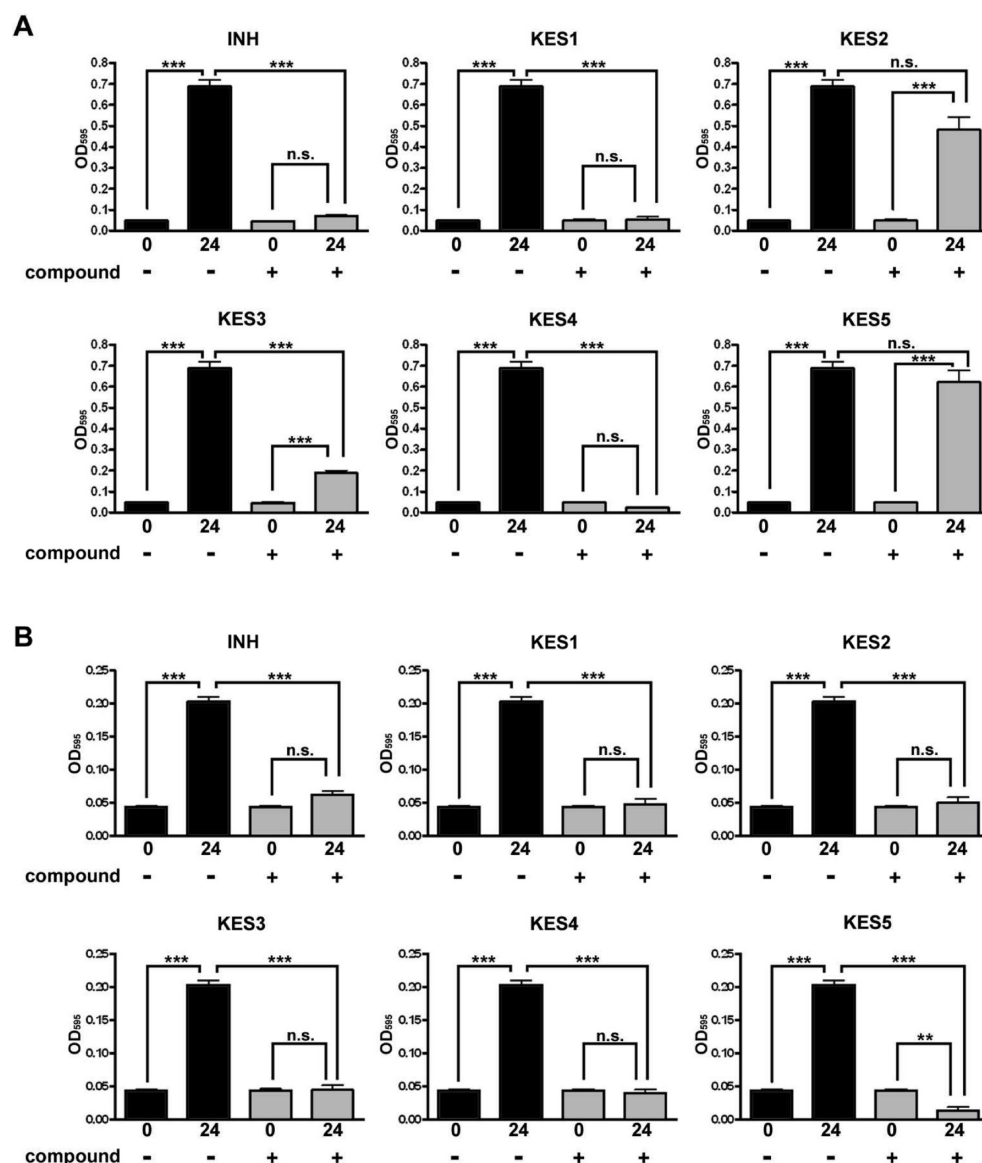


Figure 6. Short-term (24 h) inhibitory effects of the KE4 analogs (KES1–KES5) on the growth of the model mycobacteria: (A) *M. smegmatis* and (B) *M. vanbaalenii*. The chemical compounds were added to the cell cultures at a concentration of 50 μ M. DMSO (0.3%) and INH (50 μ M) were used as the negative and positive controls, respectively. Each value represents the mean \pm SEM of four independent experiments. Bonferroni's all pair comparison test was performed (n.s. not significant, ** $p < 0.01$, *** $p < 0.001$).

and its analogs (KES1–KES5), we were able to find simple relationships between the type and number of receptor–ligand interactions and the chemical activity of the compounds. With the exception of compound KES4, we found that a decrease in the number of interactions affected the chemical activity of the compound (Table 3). The lower number of interactions (H-bond or arene-H) may be responsible for the lower fitness of compounds KES1 and KES3 compared with compounds KE4 and KES4. The oxygen of the 2-furoyl group of KES4 may play an important role in the formation of the H-bond receptor and might decrease the flexibility of the compound compared with compound KE4 (Figure 11 and Table 3). Focusing on the interaction with Tyr158 is likely to be effective in the structure-based chemical design of drugs against the *M. tuberculosis* InhA. Notably, the predicted interaction residues of compound KES4 (Phe149, Tyr158, and Leu218) coincide with the important residues that are located in the binding site of the INH–NAD adduct.⁴⁰ The information obtained from the SAR analysis is

likely to be helpful for the development of more potent anti-TB chemical compounds. Moreover, it is expected that the chemical compounds identified in this study have the potential to overcome the INH-resistance problem because these chemical compounds do not interact with the mutated residues found in drug-resistant *M. tuberculosis* strains (i.e., Ile21 to Val, Ile47 to Thr, and Ser94 to Ala).⁴¹

The low LogP value of KES4 also may strongly support its inhibitory effects (Table 3). The LogP value, which is also known as the octanol–water partition coefficient, is used as an indicator of the lipophilicity and solubility of a compound and is used to predict its transport properties across cell membranes. The *Mycobacterium* strains have strong cell walls that contain mycolic acid.^{8,9} Thus, the membrane and cell wall permeability is an important factor that affects the efficacy of drugs. From the standpoint of solubility, permeability, clearance, metabolism, bioavailability, and toxicity, it has been reported that a LogP value in the range of 1 to 3 is suitable for a

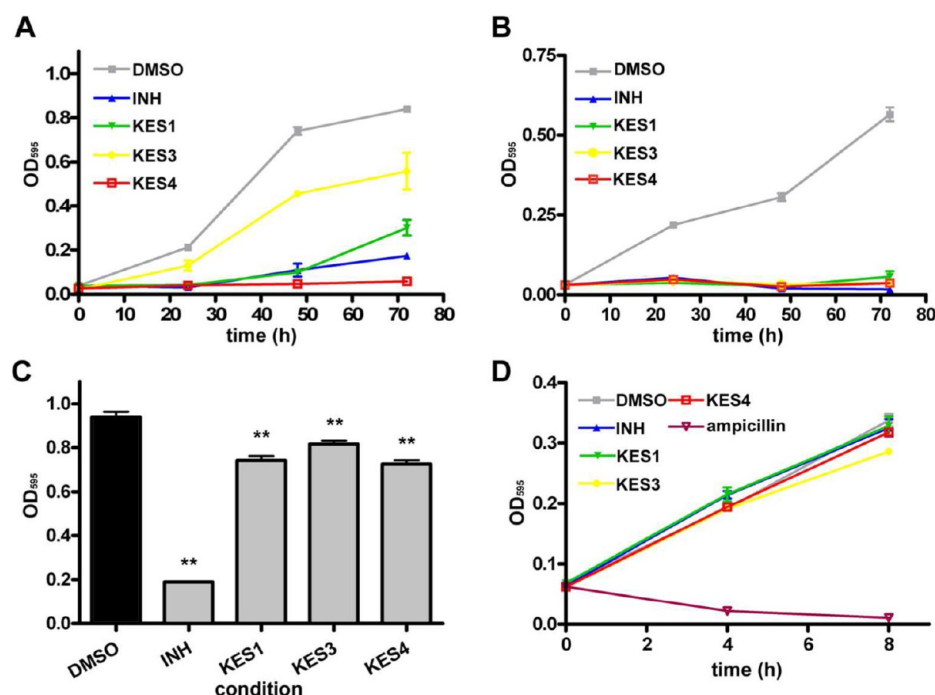


Figure 7. The effects of the KE4 analogs (KES1, KES3, and KES4) on the long-term (~ 72 h) growth of the model mycobacteria: (A) *M. smegmatis* and (B) *M. vanbaalenii*. The effects of the chemical compounds ($50 \mu\text{M}$) on the growth of (C) *R. opacus* and (D) enterobacteria (*E. coli* BL 21; ~ 8 h). The concentration of ampicillin used was $100 \mu\text{g/mL}$. DMSO (0.3%) and INH ($50 \mu\text{M}$) were used as the negative and positive controls, respectively. Each value represents the mean \pm SEM of four independent experiments. Dunnett's multiple comparison tests were performed in (D). The statistical significance is indicated (** $p < 0.01$).

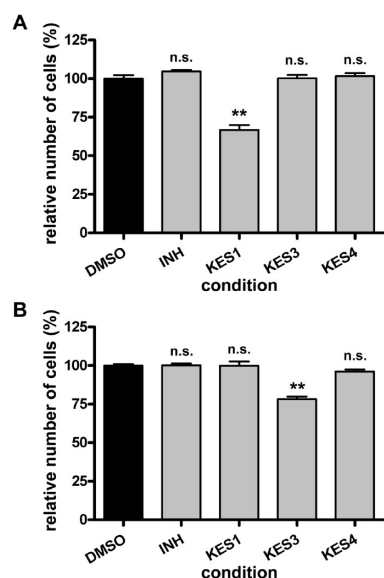


Figure 8. Toxicity of the chemical compounds (KES1, KES3, and KES4) on cultured mammalian cells: (A) MDCK and (B) SH-SY5Y cells. The chemical compounds were added to the cell cultures at a concentration of $30 \mu\text{M}$. Each value represents the mean \pm SEM of four independent experiments. Dunnett's multiple comparison tests were performed. The statistical significance is indicated (n.s. not significant, ** $p < 0.01$).

medical drug.⁴² The LogP values of each of the active hits are shown in Table 3. The LogP value of KES4 is 2.88, which is lower than the LogP values of the other active compounds (3.05–3.92). Therefore, compound KES4 is physically preferred compared with the other active compounds.

Of the 5 compounds tested, two potential chemical compounds were identified by the DOCK-GOLD hierarchical *in silico* SBDS, which resulted in a 40% hit rate. In contrast, other HTS research studies against *Mycobacterium* have obtained hit rates of 1 to 3%.^{43,44} Therefore, our SBDS strategy is considerably more efficient and effective. Moreover, it is thought that the combination of multiconformation docking, PLIF analysis, and Ligand Interaction analysis helps improve the efficiency of the drug screening.

CONCLUSION

In the present study, we performed a three-step *in silico* SBDS to identify five chemical compounds that were predicted to have high binding affinity for *M. tuberculosis* InhA. As a result of an *in vitro* biological assay, two (KE3 and KE4) of the five compounds exhibited a potent inhibitory effect. Moreover, compound KE4 exhibited no toxicity against mammalian cells and enterobacteria. In addition, all of the KE4 analogs (KES1–KES5), which were identified through a fingerprint analysis and docking simulations, also exhibited inhibitory effects against *M. smegmatis* and/or *M. vanbaalenii*. One of these compounds, KES4, had strong and stable inhibitory effects that were comparable to those obtained with INH. We found a simple correlate relationship between the activity and the type and number of the ligand-protein interactions that were identified through a SAR analysis, which was based on the binding prediction of compound KE4 and its analogs (KES1–KES5). We expect that the structural and protein–ligand interaction information will strongly support the development of more potent anti-TB chemical compounds with improved selectivity and efficacy.

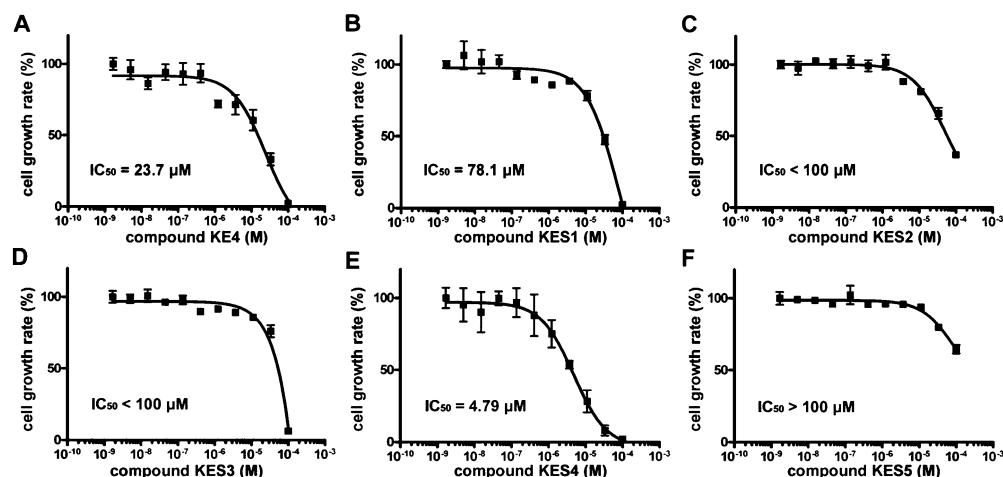


Figure 9. The dose-dependent effects of compound KE4 and compounds KES1 through KES5 on the growth of *M. smegmatis*: (A) KE4, (B) KES1, (C) KES2, (D) KES3, (E) KES4, and (F) KES5. The bacterial growth rate (%) was determined through the 24 h cultivation of *M. smegmatis*. Each plotted value represents the mean \pm SD of four independent experiments.

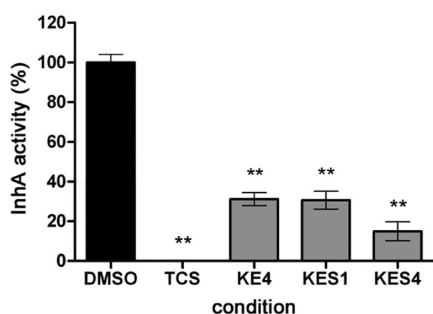


Figure 10. Effects of KE4, KES1, and KES4 on the enzymatic activity of *M. tuberculosis* InhA. The concentration of all of the chemicals was 50 μ M. DMSO (0.3%) and TCS (50 μ M) were used as negative and positive controls, respectively. The InhA enzymatic activity (%) was calculated relative to the negative control turnover rate (9.1 s⁻¹). Each value represents the mean \pm SEM of three independent experiments. Dunnett's multiple comparison test was performed (** $p < 0.01$).

MATERIALS AND METHODS

Compound Library Preparation. For the DOCK-GOLD chain screening, we used a virtual compound library (ChemBridge, 154,118 compounds) that was obtained from the Web-based chemical structure database Ressource Parisienne en Bioinformatique Structurale (RPBS).⁴⁵ The compound library was filtered using the ADME/Tox (absorption, distribution, metabolism, excretion, and toxicity) method.⁴⁶ The chemical compound library (154,118 compounds) was previously tested using the Protonate 3D module at pH 7.0. For the chemical structure similarity analysis, we generated a virtual compound library (ChemBridge, 461,397 compounds) using the stereochemistry module of MOE version 2011.10.³¹ First, the two-dimensional structures were converted into three-dimensional structures. After generating three-dimensional structures, the protonation state was treated under the same pH condition (pH 7.0) as those described above. Then, ten multi-conformations were generated from every compound using the conformation search module (LowMode MD module) of MOE.

Protein Structure Preparation. The crystal structure data of the *M. tuberculosis* InhA were obtained from the Protein Data Bank (PDB ID: 2H7I).^{47,48} For the SBDS, hydrogen atoms

were added to *M. tuberculosis* InhA using the Protonate 3D module at pH 7.0 in MOE.³¹ The partial charges of the protein structure were adjusted using the Partial Charged module, and the energy minimization of the structure was performed using the Energy Minimize module in MOE.

In Silico Structure-Based Screening. *In silico* screening experiments were performed using the UCSF DOCK (version 6.3)¹⁹ and GOLD^{21,22} programs. In the first screening, which was performed using DOCK, the interaction energy was calculated as a grid score, which is determined by its scoring function $E_{\text{int}} = E_{\text{vdw}} + E_{\text{elec}}$ (E_{int} : interaction energy, E_{vdw} : van der Waals energy, E_{elec} : electrostatic energy) against the active site of InhA. The DOCK screening of the chemical compound library (154,118 compounds) predicted the top 2,000 ranked chemical compounds. The grid scores of these compounds were estimated to be below the threshold of -49.7 kcal/mol. These chemical compounds were used in a second screening. In the second screening, we employed the GOLD program, which performs receptor–ligand docking using a genetic algorithm (GA) to explore flexible ligand conformations and allows partial receptor flexibility.²¹ Using the 2,000 chemical compounds that were identified by the first DOCK screening, we performed the GOLD screening under the following conditions: the number of individual operations was set to a minimum of 100 and a maximum of 100,000 and the number of conformations generated was set to a maximum of 10 when the RMSD of three scoring poses was higher than 1.5 Å. The GOLD program evaluates the calculated results of the protein–chemical compound hydrogen bonding energy, the van der Waals contact energy, and the torsion energy to determine the GOLD score. As a result of the second screening, the top 1,000 ranked chemical compounds (GOLD score >85) were extracted for a third screening. In the third screening, we performed a GOLD screening using multiple conformations of the top 1,000 ranked chemical compounds. As a result of the third screening, 5 unique chemical compounds were chosen by clustering using the BIT_MACCS fingerprint method^{31,33} from the top 29 ranked chemical compounds (GOLD score average >80), which were obtained based on the average GOLD scores of the multiconformation compounds.

Screening of Similar Compounds. A total of 14 chemical compounds that were similar to KE4 were chosen from the

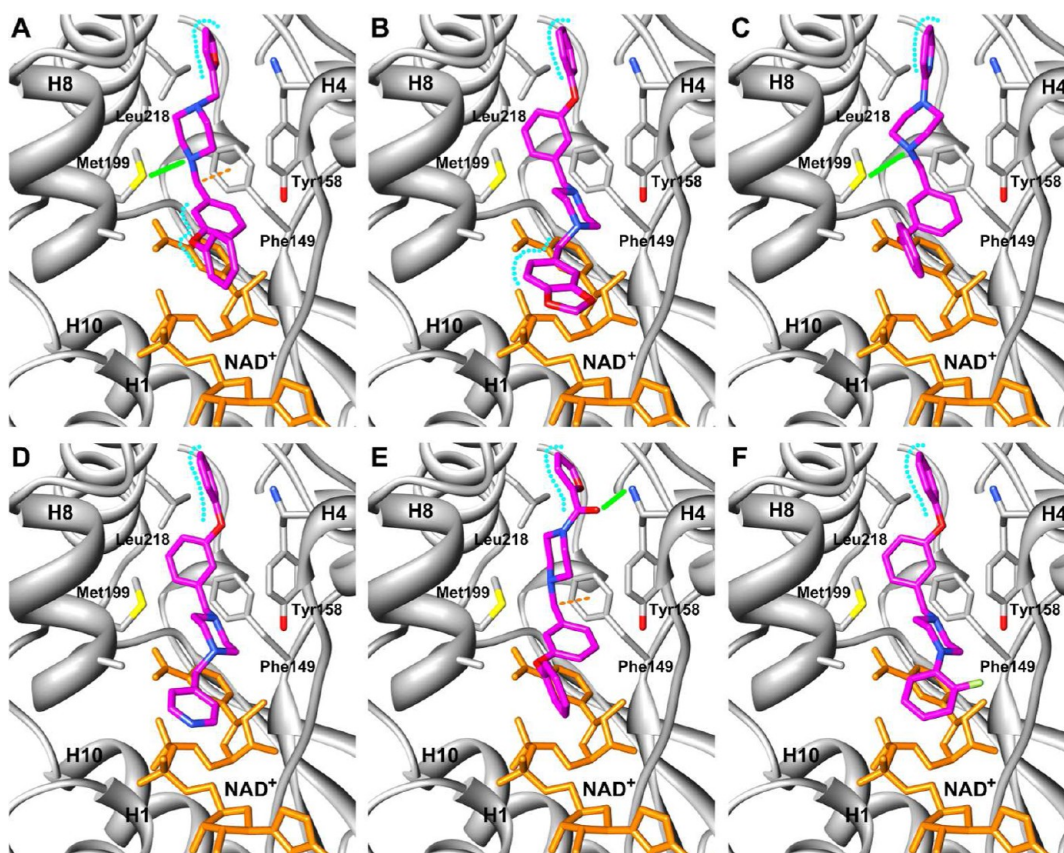


Figure 11. The predicted binding modes between the target protein and the compounds KE4 (A) and KES1–KES5 (B–F) by PLIF analysis and the analysis of the ligand interactions. The hydrogen bond, arene-H, and hydrophobic interactions are indicated by green, dashed orange, and dotted blue lines, respectively. The color of the amino acid interactions is identical to the colors of the amino acids indicated in Table 3.

Table 3. Predicted Interaction Residue, IC₅₀, and LogP of Active Compounds^a

Chemical Name	Predicted Interaction Residue	IC ₅₀ (μM) ^a	LogP
KE4	Phe149, Ala198, Met199 and/or Leu218	23.7	3.51
KES1	Ala198 and/or Leu218	78.1	3.64
KES2	Met199 and Leu218	< 100	3.05
KES3	Leu218	< 100	3.31
KES4	Phe149, Tyr158 and Leu218	4.8	2.88
KES5	Leu218	> 100	3.92

^aThe * denotes the following: each value represents the IC₅₀ value on *M. smegmatis*.

Hit2LEAD Web-based database using a similarity search tool that is available on the Web site. Moreover, 1,281 additional similar compounds were obtained from the larger-scale ChemBridge virtual compound library that contains 461,397 chemicals through a MACCS fingerprint analysis^{31,33} (Tanimoto coefficient >0.75) of the MolFilter module that is available in MOE. These 1,295 total compounds were simulated using the GOLD program. As a result, 5 similar chemical compounds with a higher GOLD score than that of KE4 were identified.

Docking Metric. ROC analysis was performed to measure docking performance using DUD-E ligands and decoys set of *M. tuberculosis* InhA.⁴⁹ The three-dimensional structures of the ligands and decoys set chemicals were generated using the

Energy Minimize and stereochemistry modules in MOE. The docking studies were performed using the same method and parameters as the first step of DOCK and the second and third steps of the GOLD screening process.

Bacterial Strains and Chemical Compounds. *M. vanbaalenii*, *M. smegmatis*, and *R. opacus* were obtained from RIKEN BioResource Center (Saitama, Japan).⁵⁰ The *E. coli* JM109 and BL21 strains were kindly gifted by Dr. S. Sueda (Kyushu Institute of Technology). The chemical compounds used in this study, which were purchased from ChemBridge (San Diego, CA, USA; supplier IDs given in parentheses), are the following:

KE1: 4,4'-[sulfonylbis(4,1-phenyleneoxy)]dianiline (S172393);

KE2: 1-[4-(benzyloxy)benzyl]-N-(4-methoxybenzyl)-4-piperidinecarboxamide oxalate (6577882);

KE3: 3-{[4-(1,3-benzodioxol-5-ylmethyl)-1-piperazinyl]-methyl}-9-ethyl-9H-carbazole (S270317);

KE4: 1-(2-furymethyl)-4-(3-phenoxybenzyl)piperazine oxalate (6569200);

KE5: 5-(2-methoxyphenoxy)-2-[4-(4-pyridinylmethyl)-phenyl]-1H-isindole-1,3(2H)-dione (6716034);

KES1: 1-(1,3-benzodioxol-5-ylmethyl)-4-(3-phenoxybenzyl)-piperazine (S257245);

KES2: 1-(3-phenoxybenzyl)-4-(2-pyridinyl)piperazine (S258489);

KES3: 1-(3-phenoxybenzyl)-4-(4-pyridinylmethyl)piperazine (S995975);

KES4: 1-(2-furoyl)-4-(3-phenoxybenzyl)piperazine oxalate (6041917); and

KES5: 1-(2-fluorophenyl)-4-(3-phenoxybenzyl)piperazine (5264989).

In Vitro Bacterial Growth Conditions and Bacterial Growth Activity Assay. The bacterial culturing was performed according to previously described methods.²⁶ *M. vanbaalenii* and *R. opacus* were incubated overnight at 300 rpm and 28 °C in 4 and 3 mL, respectively, of the corresponding culture medium [*M. vanbaalenii*: 3.7% brain heart infusion broth (Difco), *R. opacus*: 1% glucose (Wako), 0.1% L-asparagine (Wako), 0.05% K₂HPO₄ (Wako), and 0.2% yeast extract (BD)]. *M. smegmatis* and *E. coli* were incubated for two days and 18 h, respectively, at 300 rpm and 37 °C in 3 mL of the corresponding culture medium [*M. smegmatis*: 3.7% brain heart infusion broth (Difco), *E. coli*: 0.5% yeast extract (BD), 0.5% NaCl (Wako), and 1% tryptone (BD)]. We used a 6 × dilution of the *M. vanbaalenii* culture, an 8 × dilution of the *M. smegmatis* culture, and a 15 × dilution of the *R. opacus* and *E. coli* cultures for the growth experiments. The chemical compounds were dissolved in dimethyl sulfoxide (DMSO, Sigma) at a concentration of 33 mM, and the subsequent dilutions were prepared in the corresponding culture medium. The bacterial strains were seeded in 96-well assay plates and incubated in culture medium containing the specified chemical compounds. As a positive control, INH (LKT) was used in the *M. vanbaalenii*, *R. opacus* (at 28 °C and 300 rpm), and *M. smegmatis* (at 37 °C and 300 rpm) growth assays, and ampicillin (Sigma) was used for the *E. coli* growth assays (at 37 °C and 300 rpm). As a negative control, DMSO (0.3%) was used in each bacterial growth assay. After 4, 8, 18, 24, 48, and 72 h, the absorbances (595 nm) of the culture media were measured using a microplate reader (BioRad). In the long term growth assay experiments, the indicated chemical compounds (or INH as control) were added at 0, 24, and 48 h.

Mammalian Cell Toxicity Assay. MDCK and SH-SY5Y cells were used to test the mammalian cell toxicity of the chemical compounds by counting the number of cells. The cell viability was measured using the Cell Counting Kit-8 (DOJIN) by measuring the number of cells. These cells were seeded in 100-mm dishes and maintained by changing the DMEM (Wako) culture medium, which contained 10% FBS (Gibco), 2 mM L-glutamine (Gibco), 100 units/mL penicillin (Gibco), and 100 mg/mL streptomycin (Gibco). A 96-well plate was seeded with the MDCK and SH-SY5Y cells at densities of 5.0×10^3 and 1.5×10^4 cells/well, respectively, and incubated for 6 h or overnight, respectively, at 37 °C in 5% CO₂. The cell culture medium was then replaced with a 0.25% FBS medium and incubated at 37 °C in 5% CO₂. After the plates were incubated overnight (MDCK cells) or for 48 h (SH-SY5Y cells), the cell culture medium was replaced with 0.25% FBS cell culture medium containing the indicated chemical compound at a concentration of 30 μM. The cells were incubated for 24 h (MDCK cells) and 48 h (SH-SY5Y cells) at 37 °C in 5% CO₂. The following day, 10 μL of the Cell Counting Kit-8 solution was added to the culture wells, and the absorbance of formazan in the culture medium was measured at 450 nm with a microplate reader (BioRad).

Estimation of Oral LD₅₀ in Rats. Oral LD₅₀ values were predicted using the Web-based QSAR tool, TEST ver. 4.1.⁵¹ TEST is based on two-dimensional molecular descriptors using several advanced QSAR computational approaches: Hierarchical, FDA, Nearest Neighbor, etc. (USEPA, 2013). TEST

utilizes a consensus method that calculates the average of the predicted toxicities from several QSAR methodologies. It was reported that compared with single QSAR methods, the consensus method yielded the best prediction results and provided the highest prediction coverage.³⁶

Synthesis of the InhA Substrate, 2-*trans*-Decenoyl CoA. The InhA substrate, 2-*trans*-decenoyl CoA, was synthesized using previously described methods with slight modification.⁵² Briefly, 2-*trans*-decenoic acid (0.10 mmol, TCI), Coenzyme A trilithium salt (0.05 mmol, Sigma), PyBOP (0.08 mmol, Sigma), and K₂CO₃ (0.20 mmol, Sigma) were dissolved in 4 mL of THF/water (1:1) and incubated for 2 h at room temperature. After lyophilization, the resulting white solids were dissolved in water and purified with a 5C₁₈-AR-300 column (nacalai tesque) by HPLC (MILLIPORE Waters 600E) with a gradient of 10–90% acetonitrile (Wako) containing 0.04% TFA (Wako) and at a flow rate of 1.0 mL/min. Product elution was monitored at 220 nm (HITACHI L-400), and the identity of 2-*trans*-decenoyl CoA was confirmed using MALDI-TOF MS (PerSeptive Biosystems) analysis. The MALDI-TOF MS spectrum of the purified substrate showed a single peak with a molecular weight of 920.45 (data not shown).

Enzymatic Assay. The enzymatic activity of InhA was assayed using previously described methods, with slight modification.⁵³ *M. tuberculosis* InhA recombinant protein was a kind gift from Prof. J. C. Sacchettini.⁵⁴ The enzyme reactions were performed at a final volume of 100 μL in 96-well assay plates (CORNING). For the enzymatic assays, preincubation reactions were performed, with each well containing 30 mM PIPES (Sigma) buffer (pH 7.0), 70 nM *M. tuberculosis* InhA, 200 μM NADH (Sigma), 150 mM NaCl (Wako), and the candidate chemicals (KE4, KES1, and KES4 at 50 μM). Triclosan (TCI) was used as a positive control. The solution was incubated for 5 min at 25 °C. To start the enzymatic reaction, 175 μM substrate (2-*trans*-decenoyl CoA) was added to each well. The oxidation of NADH (340 nm) was measured with a thermostatic micro plate reader (TECAN SUNRISE Thermo RC spectrophotometer).

Statistical Analysis. All of the statistical analyses were performed using R version 2.15.0 (The R Foundation for Statistical Computing, Vienna, Austria) and GraphPad Prism version 4 (GraphPad Software, Inc., San Diego, CA, USA).

AUTHOR INFORMATION

Corresponding Author

*Phone: +81-948-29-7819. Fax +81-948-29-7801. E-mail: aokis@bio.kyutech.ac.jp. Corresponding author mailing address: Department of Bioscience and Bioinformatics, Graduate School of Computer Science and Systems Engineering, Kyushu Institute of Technology, 680-4 Kawazu, Iizuka-shi, Fukuoka 820-8502, Japan.

Author Contributions

[†]These authors contributed equally to this work.

Notes

The authors declare no competing financial interest.

ACKNOWLEDGMENTS

The authors are very thankful to Prof. S. Kikuchi (Muroran Institute of Technology) and Dr. S. Fujii (Kyushu Institute of Technology) for their valuable comments and to Mr. K.

Tsuruta (Kyushu Institute of Technology) for the technical support.

■ ABBREVIATIONS

SBDS, structure-based drug screening; TB, tuberculosis; MDR, multidrug-resistant; XDR, extensively drug-resistant; HIV, human immunodeficiency virus; INH, isoniazid; TCS, triclosan; HTS, high-throughput screening; QSAR, quantitative structure–activity relationship; PLIF, protein–ligand interaction fingerprint; SAR, structure–activity relationship; ROC, receiver-operating characteristic; AUC, area under the curve; RPBS, Ressource Parisienne en Bioinformatique Structurale; GA, genetic algorithm; MDCK, Madin-Darby canine kidney; SH-SY5Y, human neuroblastoma cells; DMSO, dimethyl sulfoxide; RFP, Rifampicin; TEST, Toxicity Estimation Software Tool

■ REFERENCES

- (1) World Health Organization, Global tuberculosis control: WHO report 2011, ISBN 978 92 4 156438 0.
- (2) Dye, C.; Williams, B. G. The population dynamics and control of tuberculosis. *Science* **2010**, *328*, 856–861.
- (3) Rawat, R.; Whitty, A.; Tonge, P. J. The isoniazid-NAD adduct is a slow, tight-binding inhibitor of InhA, the *Mycobacterium tuberculosis* enoyl reductase: adduct affinity and drug resistance. *Proc. Natl. Acad. Sci. U. S. A.* **2003**, *100*, 13881–13886.
- (4) Lei, B. F.; Wei, C. J.; Tu, S. C. Action mechanism of antitubercular isoniazid - activation *Mycobacterium tuberculosis* KatG, isolation, and characterization of InhA inhibitor. *J. Biol. Chem.* **2000**, *275*, 2520–2526.
- (5) Takayama, K.; Wang, C.; Besra, G. S. Pathway to synthesis and processing of mycolic acids in *Mycobacterium tuberculosis*. *Clin. Microbiol. Rev.* **2005**, *18*, 81–101.
- (6) White, S. W.; Zheng, J.; Zhang, Y. M.; Rock, C. O. The structural biology of type II fatty acid biosynthesis. *Annu. Rev. Biochem.* **2005**, *Vol. 74*, 791–831.
- (7) Lu, H.; Tonge, P. J. Inhibitors of FabI, an enzyme drug target in the bacterial fatty acid biosynthesis pathway. *Acc. Chem. Res.* **2008**, *41*.
- (8) Chatterjee, D. The mycobacterial cell wall: structure, biosynthesis and sites of drug action. *Curr. Opin. Chem. Biol.* **1997**, *1*, 579–588.
- (9) Brennan, P. J. Structure, function, and biogenesis of the cell wall of *Mycobacterium tuberculosis*. *Tuberculosis* **2003**, *83*, 91–97.
- (10) Mitchell, J. R.; Zimmerman, H. J.; Ishak, K. G.; Thorgeirsson, U. P.; Timbrell, J. A.; Snodgrass, W. R.; Nelson, S. D. Isoniazid liver-injury: clinical spectrum, pathology, and probable pathogenesis. *Ann. Intern. Med.* **1976**, *84*, 181–192.
- (11) Dobner, P.; RuschGerdes, S.; Bretzel, G.; Feldmann, K.; Rifai, M.; Loscher, T.; Rinder, H. Usefulness of *Mycobacterium tuberculosis* genomic mutations in the genes katG and inhA for the prediction of isoniazid resistance. *Int. J. Tuberc. Lung Dis.* **1997**, *1*, 365–369.
- (12) Musser, J. M.; Kapur, V.; Williams, D. L.; Kreiswirth, B. N.; van Soolingen, D.; van Embden, J. D. A. Characterization of the catalase-peroxidase gene (katG) and inhA locus in isoniazid-resistant and -susceptible strains of *Mycobacterium tuberculosis* by automated DNA sequencing: restricted array of mutations associated with drug resistance. *J. Infect. Dis.* **1996**, *173*, 196–202.
- (13) Suarez, J.; Rangelova, K.; Jarzecki, A. A.; Manzerova, J.; Krymov, V.; Zhao, X.; Yu, S.; Metlitsky, L.; Gerfen, G. J.; Magliozzo, R. S. An oxyferrous heme/protein-based radical intermediate is catalytically competent in the catalase reaction of *Mycobacterium tuberculosis* catalase-peroxidase (KatG). *J. Biol. Chem.* **2009**, *284*.
- (14) Hansch, C.; Muir, R. M.; Fujita, T.; Maloney, P. P.; Geiger, F.; Streich, M. The correlation of biological activity of plant growth regulators and chloromycetin derivatives with hammett constants and partition coefficients. *J. Am. Chem. Soc.* **1963**, *85* (18), 2817–2824.
- (15) Langer, T.; Wolber, G. Pharmacophore definition and 3D searches. *Drug Discovery Today: Technol.* **2004**, *1* (3), 203–207.
- (16) Bender, A.; Mussa, H. Y.; Glen, R. C.; Reiling, S. Similarity searching of chemical databases using atom environment descriptors (MOLPRINT 2D): evaluation of performance. *J. Chem. Inf. Comput. Sci.* **2004**, *44*, 1708–1718.
- (17) van Geerestein, V. J.; Perry, N. C.; Grootenhuys, P. D. J.; Haasnoot, C. A. G. 3D database searching on the basis of ligand shape using the prototype method. *Tetrahedron Comput. Methodol.* **1990**, *595*–613.
- (18) Lengauer, T.; Rarey, M. Computational methods for biomolecular docking. *Curr. Opin. Struct. Biol.* **1996**, *6*, 402–406.
- (19) Lang, P. T.; Brozell, S. R.; Mukherjee, S.; Pettersen, E. F.; Meng, E. C.; Thomas, V.; Rizzo, R. C.; Case, D. A.; James, T. L.; Kuntz, I. D. DOCK 6: combining techniques to model RNA-small molecule complexes. *RNA* **2009**, *15*, 1219–1230.
- (20) Goodsell, D. S.; Olson, A. J. Automated docking of substrates to proteins by simulated annealing. *Proteins* **1990**, *8* (3), 195–202.
- (21) Jones, G.; Willett, P.; Glen, R. C. Molecular recognition of receptor sites using a genetic algorithm with a description of desolvation. *J. Mol. Biol.* **1995**, *245*, 43–53.
- (22) Jones, G.; Willett, P.; Glen, R. C.; Leach, A. R.; Taylor, R. Development and validation of a genetic algorithm for flexible docking. *J. Mol. Biol.* **1997**, *267*, 727–748.
- (23) Friesner, R. A.; Banks, J. L.; Murphy, R. B.; Halgren, T. A.; Klicic, J. J.; Mainz, D. T.; Repasky, M. P.; Knoll, E. H.; Shelley, M.; Perry, J. K.; Shaw, D. E.; Francis, P.; Shenkin, P. S. Glide: a new approach for rapid, accurate docking and scoring. 1. Method and assessment of docking accuracy. *J. Med. Chem.* **2004**, *47* (7), 1739–1749.
- (24) Hirayama, K.; Aoki, S.; Nishikawa, K.; Matsumoto, T.; Wada, K. Identification of novel chemical inhibitors for ubiquitin C-terminal hydrolase-L3 by virtual screening. *Bioorg. Med. Chem.* **2007**, *15*, 6810–6818.
- (25) Mitsui, T.; Hirayama, K.; Aoki, S.; Nishikawa, K.; Uchida, K.; Matsumoto, T.; Kabuta, T.; Wada, K. Identification of a novel chemical potentiator and inhibitors of UCH-L1 by *in silico* drug screening. *Neurochem. Int.* **2010**, *56*, 679–686.
- (26) Izumizono, Y.; Arevalo, S.; Koseki, Y.; Kuroki, M.; Aoki, S. Identification of novel potential antibiotics for tuberculosis by *in silico* structure-based drug screening. *Eur. J. Med. Chem.* **2011**, *46*, 1849–1856.
- (27) Koseki, Y.; Kinjo, T.; Kobayashi, M.; Aoki, S. Identification of novel antimycobacterial chemical agents through the *in silico* multi-conformational structure-based drug screening of a large-scale chemical library. *Eur. J. Med. Chem.* **2013**, *60*, 333–339.
- (28) ChemBridge. <http://www.chembridge.com> (accessed March 28, 2013).
- (29) Rozwarski, D. A.; Vilcheze, C.; Sugantino, M.; Bittman, R.; Sacchettini, J. C. Crystal structure of the *Mycobacterium tuberculosis* enoyl-ACP reductase, InhA, in complex with NAD(+) and a C16 fatty acyl substrate. *J. Biol. Chem.* **1999**, *274*, 15582–15589.
- (30) Luckner, S. R.; Liu, N.; Ende, C. W. A.; Tonge, P. J.; Kisker, C. A slow, tight binding inhibitor of InhA, the enoyl-acyl carrier protein reductase from *Mycobacterium tuberculosis*. *J. Biol. Chem.* **2010**, *285*, 14330–14337.
- (31) Molecular Operating Environment (MOE), 2010.10; Chemical Computing Group Inc., 1010 Sherbooke St. West, Suite #910, Montreal, QC, Canada, H3A 2R7, 2010.
- (32) Labute, P. LowModeMD-implicit low-mode velocity filtering applied to conformational search of macrocycles and protein loops. *J. Chem. Inf. Model.* **2010**, *50*, 792–800.
- (33) McGregor, M. J.; Pallai, P. V. Clustering of large databases of compounds: using the MDL “keys” as structural descriptors. *J. Chem. Inf. Comput. Sci.* **1997**, *37*, 443–448.
- (34) Johnson, M.; Zaretskaya, I.; Raytsel, Y.; Merezuk, Y.; McGinnis, S.; Madden, T. L. NCBIBLAST: a better web interface. *Nucleic Acids Res.* **2008**, *36*, W5–W9.
- (35) Koul, A.; Arnoult, E.; Lounis, N.; Guillemont, J.; Andries, K. The challenge of new drug discovery for tuberculosis. *Nature* **2011**, *469*, 483–490.

- (36) Zhu, H.; Martin, T. M.; Ye, L.; Sedykh, A.; Young, D. M.; Tropsha, A. Quantitative structure-activity relationship modeling of rat acute toxicity by oral exposure. *Chem. Res. Toxicol.* **2009**, *22*, 1913–1921.
- (37) Parikh, S. L.; Xiao, G. P.; Tonge, P. J. Inhibition of InhA, the enoyl reductase from *Mycobacterium tuberculosis*, by triclosan and isoniazid. *Biochemistry* **2000**, *39*, 7645–7650.
- (38) Banerjee, A.; Dubnau, E.; Quemard, A.; Balasubramanian, V.; Um, K. S.; Wilson, T.; Collins, D.; Delisle, G.; Jacobs, W. R. InhA, a gene encoding a target for isoniazid and ethionamide in *Mycobacterium tuberculosis*. *Science* **1994**, *263*, 227–273.
- (39) Aldridge, B. B.; Fernandez-Suarez, M.; Heller, D.; Ambravaneswaran, V.; Irimia, D.; Toner, M.; Fortune, S. M. Asymmetry and aging of mycobacterial cells lead to variable growth and antibiotic susceptibility. *Science* **2012**, *335*, 100–104.
- (40) Dias, M. V. B.; Vasconcelos, I. B.; Prado, A. M. X.; Fadel, V.; Basso, L. A.; De Azevedo, W. F., Jr.; Santos, D. S. Crystallographic studies on the binding of isonicotinyl-NAD adduct to wild-type and isoniazid resistant 2-*trans*-enoyl-ACP (CoA) reductase from *Mycobacterium tuberculosis*. *J. Struct. Biol.* **2007**, *159*, 369–380.
- (41) Oliveira, J. S.; Pereira, J. H.; Canduri, F.; Rodrigues, N. C.; de Souza, O. N.; de Azevedo, W. F.; Basso, L. A.; Santos, D. S. Crystallographic and pre-steady-state kinetics studies on binding of NADH to wild-type and isoniazid-resistant enoyl-ACP (CoA) reductase enzymes from *Mycobacterium tuberculosis*. *J. Mol. Biol.* **2006**, *359*, 646–666.
- (42) Waring, M. J. Lipophilicity in drug discovery. *Expert Opin. Drug Discovery* **2010**, *5*, 235–248.
- (43) Maddry, J. A.; Ananthan, S.; Goldman, R. C.; Hobrath, J. V.; Kwong, C. D.; Maddox, C.; Rasmussen, L.; Reynolds, R. C.; Secrist, J. A., III; Sosa, M. I.; White, E. L.; Zhang, W. Antituberculosis activity of the molecular libraries screening center network library. *Tuberculosis* **2009**, *89*, 354–363.
- (44) Ananthan, S.; Faaleolea, E. R.; Goldman, R. C.; Hobrath, J. V.; Kwong, C. D.; Laughon, B. E.; Maddry, J. A.; Mehta, A.; Rasmussen, L.; Reynolds, R. C.; Secrist, J. A., III; Shindo, N.; Showe, D. N.; Sosa, M. I.; Suling, W. J.; White, E. L. High-throughput screening for inhibitors of *Mycobacterium tuberculosis* H37Rv. *Tuberculosis* **2009**, *89*, 334–353.
- (45) RPBS. http://bioserv.rpbs.jussieu.fr/RPBS/cgi-bin/Ressource.cgi?chzn_lg=an&chzn_rsrc=Collections (accessed March 28, 2013).
- (46) Lipinski, C. A. Drug-like properties and the causes of poor solubility and poor permeability. *J. Pharmacol. Toxicol. Methods* **2000**, *44*, 235–249.
- (47) He, X.; Alian, A.; Stroud, R.; de Montellano, P. R. O. Pyrrolidine carboxamides as a novel class of inhibitors of enoyl acyl carrier protein reductase from *Mycobacterium tuberculosis*. *J. Med. Chem.* **2006**, *49*.
- (48) Berman, H. M.; Westbrook, J.; Feng, Z.; Gilliland, G.; Bhat, T. N.; Weissig, H.; Shindyalov, I. N.; Bourne, P. E. The Protein Data Bank. *Nucleic Acids Res.* **2000**, *28*, 235–242.
- (49) Mysinger, M. M.; Carchia, M.; Irwin, J. J.; Shoichet, B. K. Directory of useful decoys, enhanced (DUD-E): better ligands and decoys for better benchmarking. *J. Med. Chem.* **2012**, *55*, 6582–6594.
- (50) RIKEN, RIKEN BioResource Center. <http://www.jcm.riken.go.jp> (accessed March 28, 2013).
- (51) TEST. <http://www.epa.gov/nrmrl/std/qsar/qsar.html> (accessed March 28, 2013).
- (52) Kopp, F.; Linne, U.; Oberthur, M.; Marahiel, M. A. Harnessing the chemical activation inherent to carrier protein-bound thioesters for the characterization of lipopeptide fatty acid tailoring enzymes. *J. Am. Chem. Soc.* **2008**, *130*, 2656–2666.
- (53) Delaine, T.; Bernardes-Genisson, V.; Quemard, A.; Constant, P.; Meunier, B.; Bernadou, J. Development of isoniazid-NAD truncated adducts embedding a lipophilic fragment as potential bi-substrate InhA inhibitors and antimycobacterial agents. *Eur. J. Med. Chem.* **2010**, *45*, 4554–4561.
- (54) Molle, V.; Gulten, G.; Vilcheze, C.; Veyron-Churlet, R.; Zanella-Cleon, I.; Sacchettini, J. C.; Jacobs, W. R., Jr.; Kremer, L. Phosphorylation of InhA inhibits mycolic acid biosynthesis and growth of *Mycobacterium tuberculosis*. *Mol. Microbiol.* **2010**, *78*, 1591–1605.